

Emergent symmetries in atomic nuclei: Probing nuclear dynamics and physics beyond the standard model

K. D. Launey^{1*}, K. S. Becker¹, G. H. Sargsyan^{1,2}, O. M. Molchanov¹, M. Burrows¹, A. Mercenne¹, T. Dytrych^{1,3}, D. Langr⁴ and J. P. Draayer¹

¹ Department of Physics and Astronomy, Louisiana State University, Baton Rouge, LA 70803, USA

² Lawrence Livermore National Laboratory, Livermore, California 94550, USA

³ Nuclear Physics Institute of the Czech Academy of Sciences, 250 68 Řež, Czech Republic

⁴ Department of Computer Systems, Faculty of Information Technology, Czech Technical University in Prague, 16000 Praha, Czech Republic

* klauney@lsu.edu

March 10, 2023

1

2



34th International Colloquium on Group Theoretical Methods in Physics
Strasbourg, 18-22 July 2022
doi:[10.21468/SciPostPhysProc.7.1.000](https://doi.org/10.21468/SciPostPhysProc.7.1.000)

Abstract

Dominant shapes naturally emerge in atomic nuclei from first principles, thereby establishing the shape-preserving symplectic $\text{Sp}(3, \mathbb{R})$ symmetry as remarkably ubiquitous and almost perfect symmetry in nuclei. We discuss the critical role of this emergent symmetry in enabling machine-learning descriptions of heavy nuclei, *ab initio* modeling of α clustering and collectivity, as well as tests of beyond-the-standard-model physics. In addition, the $\text{Sp}(3, \mathbb{R})$ and $\text{SU}(3)$ symmetries provide relevant degrees of freedom that underpin the *ab initio* symmetry-adapted no-core shell model with the remarkable capability of reaching nuclei and reaction fragments beyond the lightest and close-to-spherical species.

13

Contents

15	1 Introduction	2
16	2 Emergent symmetries in nuclei: $\text{Sp}(3, \mathbb{R})$ and $\text{SU}(3)$	3
17	2.1 $\text{SU}(3)$ scheme	3
18	2.2 $\text{Sp}(3, \mathbb{R})$ scheme	4
19	2.3 <i>Ab initio</i> symmetry-adapted no-core shell model	7
20	3 Critical Role of Symmetries for Studies and Predictions of Nuclear Properties	8
21	3.1 Machine learning pattern recognition with the SA-NCSM	8
22	3.2 Probing clustering and physics beyond the standard model	9
23	3.3 Optical potential in the symmetry-adapted framework for nuclear reactions	10
24	4 Conclusion	11

References

12

1 Introduction

Dominant shapes, often very few in number, naturally emerge in atomic nuclei¹. This remarkable result has been recently shown by large-scale nuclear simulations from first principles [2]. Indeed, each nuclear shape respects an exact symmetry, namely, the symplectic $\text{Sp}(3, \mathbb{R})$ symmetry [3, 4]. Thereby the outcome of these simulations establishes the symplectic $\text{Sp}(3, \mathbb{R})$ symmetry as remarkably ubiquitous and almost perfect symmetry in nuclei up through the calcium region (anticipated to hold even stronger in heavy nuclei [5]). This outcome also exposes for the first time the fundamental role of the $\text{Sp}(3, \mathbb{R})$ symmetry and suggests that its origin is rooted in the strong nuclear force, in the low-energy regime.

This builds upon a decades-long research, starting with the pivotal work of Draayer [6, 4, 7, 8] and that of Rowe and Rosensteel [3, 9, 5, 10], who have successfully harnessed group theory as a powerful tool for understanding and computing the intricate structure of nuclei. This pioneering work has been instrumental in designing the theory that underpins many highly ordered patterns unveiled amidst the large body of experimental data [11, 12, 13]. In addition, it has explained phenomena observed in energy spectra, $E2$ transitions and deformation, giant resonances (GR), scissor modes and $M1$ transitions, electron scattering form factors, as well as the interplay of pairing with collectivity. The new developments and insights have provided the critical structure raised upon the very foundation laid by Elliott [14, 15, 16] and Hecht [17, 18], and opened the path for large-scale calculations feasible today on supercomputers. And while these earlier algebraic models have been very successful in explaining dominant nuclear patterns, they have assumed symmetry-based approximations and have often neglected symmetry mixing. This establishes $\text{Sp}(3, \mathbb{R})$ as an *effective symmetry*² for nuclei, which may or may not be badly broken in realistic calculations. It is then imperative to probe if this symmetry naturally arises within an *ab initio* framework, which will, in turn, establish its fundamental role.

Indeed, within an *ab initio* framework without *a priori* symmetry assumptions, the symmetry-adapted no-core shell model (SA-NCSM) [20, 21, 8] with chiral effective field theory (EFT) interactions [22, 23, 24] has recently confirmed the goodness of the symplectic $\text{Sp}(3, \mathbb{R})$ symmetry that is only slightly broken. With no parameters to adjust, the SA-NCSM is capable then not only to explain but also to predict the emergence of nuclear shapes and collectivity across nuclei, even in close-to-spherical nuclear states without any recognizable rotational properties.

Within an *ab initio* framework, the emergent symmetries play a critical role, as they can inform relevant degrees of freedom. In particular, a symmetry-adapted many-body basis can be employed, as in the SA-NCSM, thereby providing solutions for drastically reduced sizes of the spaces in which particles reside (referred to as “model spaces”) compared to the corresponding ultra-large model spaces, without compromising the accuracy of results for various nuclear observables. By exploiting symplectic symmetry, *ab initio* descriptions of spherical and deformed nuclei up through the calcium region are now possible without the use of effec-

¹ This publication reuses some material from [1] under the terms of its CC BY license.

² A familiar example for an effective symmetry is $\text{SU}(3)$. While the Elliott model with a single $\text{SU}(3)$ irrep explains ground-state rotational states in deformed nuclei, the $\text{SU}(3)$ symmetry is, in general, largely mixed, mainly due to the spin-orbit interaction (nonetheless, $\text{SU}(3)$ has been shown to be an excellent quasi-dynamical symmetry, that is, each rotational state has almost the same $\text{SU}(3)$ content [19]).

tive charges [21, 25, 26, 8, 27]. This allows the SA-NCSM to accommodate even larger model spaces and to reach heavier nuclei, such as ^{20}Ne [2], ^{21}Mg [28], ^{22}Mg [29], ^{28}Mg [30], as well as ^{32}Ne and ^{48}Ti [31].

In this paper, we briefly outline the $\text{SU}(3)$ and $\text{Sp}(3, \mathbb{R})$ schemes utilized by the *ab initio* SA-NCSM. We overview the critical role of the emergent $\text{Sp}(3, \mathbb{R})$ symmetry in enabling machine-learning descriptions of heavy nuclei [32], *ab initio* modeling of α clustering and collectivity, along with tests of beyond-the-standard-model physics [33]. In addition, we show that with the help of the SA-NCSM, which expands *ab initio* applications up to medium-mass nuclei by using the dominant symmetry of nuclear dynamics, one can provide solutions to reaction processes in this region, with a focus on elastic neutron scattering.

2 Emergent symmetries in nuclei: $\text{Sp}(3, \mathbb{R})$ and $\text{SU}(3)$

2.1 $\text{SU}(3)$ scheme

It is well known that $\text{SU}(3)$ [14, 34, 6, 35, 18] is the symmetry group of the spherical harmonic oscillator (HO) that underpins the valence-shell model and the valence-shell $\text{SU}(3)$ (Elliott) model [14, 15, 16] (for technical details of $\text{SU}(3)$, see Ref. [36]). The Elliott model has been shown to naturally describe rotations of a deformed nucleus without the need for breaking rotational symmetry. But even beyond the valence shell, the $\text{SU}(3)$ scheme provides a classification of the complete shell-model space in multiple shells, and is related to the LS -coupling and jj -coupling schemes via a unitary transformation. It divides the space into basis states of definite $(\lambda\mu)$ quantum numbers of $\text{SU}(3)$ that are linked to the intrinsic quadrupole deformation according to the established mapping [37, 38, 39]. For example, the simplest cases, (00) , $(\lambda 0)$, and (0μ) , describe spherical, prolate, and oblate deformation, respectively³, while a general nuclear state is typically a superposition of several hundred various triaxially deformed configurations. Note that, in this respect, basis states can have little to no deformation, and, e.g., about 60% of the ground state of the closed-shell ^{16}O is described by a single $\text{SU}(3)$ basis state, the spherical (00) .

Specifically, in the $\text{SU}(3)$ scheme, in place of the spherical quantum numbers $|\eta l m_l\rangle$, one can consider the single-particle HO basis $|\eta_z \eta_x \eta_y\rangle$, the HO quanta in the three Cartesian directions, z , x , and y , with $\eta_x + \eta_y + \eta_z = \eta$ ($\eta = 0, 1, 2, \dots$ for s, p, sd, \dots shells). For a given HO major shell, the complete shell-model space is then specified by all distinguishable distributions of η_z, η_x and η_y . E.g., for $\eta = 2$, there are 6 different distributions, $(\eta_z, \eta_x, \eta_y) = (2, 0, 0), (1, 1, 0), (1, 0, 1), (0, 2, 0), (0, 1, 1)$ and $(0, 0, 2)$. The number of these configurations is $\Omega_\eta = (\eta + 1)(\eta + 2)/2$ (spatial degeneracy) and the associated symmetry is described by the $U(\Omega_\eta)$ unitary group. Each of these (η_z, η_x, η_y) configurations can be either unoccupied or has maximum of two particles with spins $\uparrow\downarrow$.

As a simple example for an $\text{SU}(3)$ -scheme basis state, consider $A = 2$ protons in the sd shell ($\eta = 2$) with a particle in the $(2, 0, 0)$ level with spin \uparrow and another in the $(1, 1, 0)$ level with spin \uparrow . The total number of quanta in each direction is $(\eta_z^{\text{tot}}, \eta_x^{\text{tot}}, \eta_y^{\text{tot}}) = (3, 1, 0)$, or equivalently, $\eta^{\text{tot}}(\lambda\mu) = 4(21)$, where $\eta^{\text{tot}} = \eta_x^{\text{tot}} + \eta_y^{\text{tot}} + \eta_z^{\text{tot}}$, together with $\lambda = \eta_z^{\text{tot}} - \eta_x^{\text{tot}}$ and $\mu = \eta_x^{\text{tot}} - \eta_y^{\text{tot}}$ labeling an $\text{SU}(3)$ irrep, in addition to the total intrinsic spin and its projection SM_S . For given $(\lambda\mu)$, the quantum numbers κ , L and M_L are given by Elliott [14, 15], according to the $\text{SU}(3) \supset \text{SO}(3)_L \supset \text{SO}(2)_{M_L}$, where the label κ distinguishes multiple occurrences of the same orbital angular momentum L in the parent irrep $(\lambda\mu)$. For our

³ Following this mapping, quadrupole moments of (00) , $(\lambda 0)$, and (0μ) configurations – in a simple classical analogy to rotating spherical, prolate, and oblate spheroids in the lab frame [40] – are zero, negative, and positive, respectively.

example, $(\lambda\mu) = (2\ 1)$ with $\kappa = 1$, $L = 1, 2, 3$, and $M_L = -L, -L+1, \dots, L$. Hence, the set $\{\eta^A(\lambda\mu)\kappa(LS)JM\}$ completely labels a 2-proton SU(3)-scheme basis state (with $\eta^{\text{tot}} = A\eta$). A basis state in this scheme for a 2-particle system is given by, $\{a_{(\eta 0)st_z}^\dagger \times a_{(\eta' 0)s't'_z}^\dagger\}^{(\lambda\mu)\kappa(LS)JM} |0\rangle$, which is an SU(3)-coupled product, provided that a^\dagger is a proper SU(3) tensor; incidentally, the SU(3) tensor a^\dagger of rank $(\lambda\mu) = (\eta 0)$ coincides with the familiar particle creation operator, $a_{(\eta 0)lms\sigma t_z}^\dagger \equiv a_{\eta lms\sigma t_z}^\dagger$, while the particle annihilation SU(3) tensor of rank $(\lambda\mu) = (0\ \eta)$ is given as $\tilde{a}_{(0\eta)l-ms-\sigma t_z} = (-1)^{\eta+l-m+s-\sigma} a_{\eta lms\sigma t_z}$. Note that for $\eta = \eta' = 2$, e.g., there are only a few 2-proton configurations $(\lambda\mu) = (4\ 0)$ with $L = 0, 2, 4$, $(2\ 1)$ with $L = 1, 2, 3$, and $(0\ 2)$ with $L = 0, 2$. Furthermore, these basis states are related to LS -coupled basis states (similarly, to jj -coupled basis states) via a simple unitary transformation,

$$\{a_{(\eta 0)st_z}^\dagger \times a_{(\eta' 0)s't'_z}^\dagger\}^{(\lambda\mu)\kappa(LS)JM} |0\rangle = \sum_{l,l'} \langle (\eta 0)l; (\eta' 0)l' | (\lambda\mu)\kappa L \rangle \{a_{\eta lst_z}^\dagger \times a_{\eta' l's't'_z}^\dagger\}^{(LS)JM} |0\rangle, \quad (1)$$

where $\langle \dots; \dots | \dots \rangle$ is the SU(3) analog of the familiar reduced Clebsch-Gordan coefficient [note that there is no dependence on the particle orbital angular momenta, l and l' , in the SU(3)-scheme basis states].

An important feature of the SU(3) scheme is that all possible configurations within a major HO shell η (for protons or neutrons) are not constructed using the tedious procedure of coupling of creation operators referenced above, but are readily available based on the $U(\Omega_\eta)$ unitary group of the many-body three-dimensional HO. In particular, the basis construction is implemented according to the reduction [41]

$$\begin{array}{c} U(\Omega_\eta) \\ [f_1, f_2, \dots, f_{\Omega_\eta}] \\ \cup \\ SU(3) \\ (\lambda_\eta \mu_\eta) \end{array} \quad \alpha_\eta \quad \times \quad \begin{array}{c} SU(2) \\ S_\eta \end{array}, \quad (2)$$

with $SU(3)_{(\lambda_\eta \mu_\eta)} \supset SO(3)_{L_\eta} \supset SO(2)_{M_{L_\eta}}$ [14, 15], where a multiplicity index α_η distinguishes multiple occurrences of an SU(3) irrep $(\lambda_\eta \mu_\eta)$ in a given $U(\Omega_\eta)$ irrep labeled by Young tableaux, $[f] = [f_1, f_2, \dots, f_{\Omega_\eta}]$, with $f_1 \geq f_2 \geq \dots \geq f_{\Omega_\eta}$ and $f_i = 0$ (unoccupied), 1 (occupied by a particle), or 2 (occupied by 2 particles of spins $\uparrow\downarrow$). An illustrative example for 4 particles in the pf shell ($\eta = 3$) is shown in Table 1.

2.2 $Sp(3, \mathbb{R})$ scheme

The key role of deformation in nuclei and the coexistence of low-lying quantum states in a single nucleus characterized by configurations with different quadrupole moments [11] makes the quadrupole moment a dominant fundamental property of the nucleus. Hence, the quadrupole moment Q (or deformation) and the monopole moment r^2 (or “size” of the nucleus), along with nuclear masses, establishes the energy scale of the nuclear problem. Indeed, the nuclear monopole and quadrupole moments underpin the essence of symplectic $Sp(3, \mathbb{R})$ symmetry.

Specifically, for A particles in three-dimensional space, the complete basis for the shell model is described by $Sp(3A, \mathbb{R}) \times U(4)$ [10], where $Sp(3A, \mathbb{R})$ is the group of all linear canonical transformations of the $3A$ -particle phase space and Wigner’s supermultiplet group $U(4)$ describes the complementary spin-isospin space. A complete translationally invariant shell-

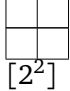
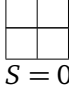
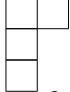
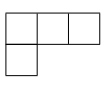

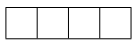
Spatial d.o.f.		Spin d.o.f.
$U(10)$ $[f_1 f_2 \dots f_{10}]$	$\supset SU(3)$ $(\lambda \mu)$	$SU(2)$ S
	$(8\ 2), (7\ 1), (4\ 4)^2, (5\ 2), (0\ 6), (6\ 0), (3\ 3)$ $(1\ 4), (4\ 1), (2\ 2)^2, (1\ 1)$	 $S = 0$
	$(9\ 0), (6\ 3), (7\ 1), (4\ 4), (2\ 5), (5\ 2)^2, (3\ 3)^2$ $(1\ 4)^2, (4\ 1)^2, (2\ 2), (0\ 3), (3\ 0)^2, (1\ 1)$	 $S = 1$
	$(5\ 2), (0\ 6), (3\ 3), (2\ 2), (3\ 0)$	 $S = 2$

Table 1: $SU(3) \times SU(2)_S$ configurations for 4 protons (neutrons) in the pf shell ($\eta = 3$ with $\Omega_\eta = 10$). Note that a spatial symmetry represented by a Young tableau $[f_1, \dots, f_{\Omega_\eta}]$ is uniquely determined by its complementary spin symmetry of a given intrinsic spin S_η (conjugate Young tableaux) ensuring the overall antisymmetrization of each $U(\Omega_\eta) \times SU(2)_{S_\eta}$ configuration with respect to spatial and spin degrees of freedom (d.o.f.) [41].

145 model basis is classified according to (see, e.g., [5, 10]),

$$\begin{array}{ccc} \text{Sp}(3(A-1), \mathbb{R}) & \times & U(4) \\ \cup & & \cup \\ \text{Sp}(3, \mathbb{R}) \times O(A-1) & & SU(2)_S \times SU(2)_T \end{array} \quad (3)$$

146 The $\text{Sp}(3, \mathbb{R})$ scheme utilizes the symplectic group $\text{Sp}(3, \mathbb{R})$. It consists of all *particle-independent*
147 linear canonical transformations of the single-particle phase-space observables, the positions
148 \vec{r}_i and momenta \vec{p}_i (with particle index $i = 1, \dots, A$ and spacial directions $\alpha, \beta = x, y, z$)

$$r'_{i\alpha} = \sum_{\beta} A_{\alpha\beta} r_{i\beta} + B_{\alpha\beta} p_{i\beta} \quad (4)$$

$$p'_{i\alpha} = \sum_{\beta} C_{\alpha\beta} r_{i\beta} + D_{\alpha\beta} p_{i\beta} \quad (5)$$

149 that preserve the Heisenberg commutation relations $[r_{i\alpha}, p_{j\beta}] = i\hbar \delta_{ij} \delta_{\alpha\beta}$ [5, 42, 8]. Genera-
150 tors of these transformations, symbolically denoted as matrices **A**, **B**, **C**, and **D**, are constructed
151 as “quadratic coordinates” in phase space, \vec{r}_i and \vec{p}_i , and, most importantly, sum over all the
152 particles and act on the space orientation. Hence, the generators include physically relevant
153 operators: the total kinetic energy ($\frac{p^2}{2} = \frac{1}{2} \sum_i \vec{p}_i \cdot \vec{p}_i$), the monopole moment ($r^2 = \sum_i \vec{r}_i \cdot \vec{r}_i$),
154 the quadrupole moment ($Q_{2M} = \sqrt{16\pi/5} \sum_i r_i^2 Y_{2M}(\hat{r}_i)$), the orbital angular momentum
155 ($\vec{L} = \sum_i \vec{r}_i \times \vec{p}_i$), and the many-body harmonic oscillator Hamiltonian ($H_0 = \frac{p^2}{2} + \frac{r^2}{2}$). In
156 addition, other generators describe multi-shell collective vibrations and vorticity degrees of
157 freedom for a description from irrotational to rigid rotor flows.

On the contrary, the generators of the complementary $O(A)$ sum over the three spatial directions and act on the particle index, with a growing complexity with increasing particle number. One can then organize the A -particle model space according to the dual group $O(A-1)$, with $O(A) \supset O(A-1) \supset S_A$. The $O(A)$ is the group of orthogonal transformations that act on the “particle-index” space (transformations of nucleon coordinates, $r_{i\alpha} \rightarrow \sum_{j=1}^A r_{j\alpha} P_{ji}$, that leave the $O(A)$ scalars $r_\alpha \cdot r_\beta = \sum_{i=1}^A r_{i\alpha} r_{i\beta}$ invariant for $\alpha, \beta = x, y, z$). This scheme is reviewed in detail in Refs. [5, 10]. $O(A-1)$ is the subgroup of $O(A)$ which leaves center-of-mass coordinates invariant (note that center-of-mass coordinates are symmetric with respect to nucleon indices and, therefore, invariant under S_A permutations) and has as a subgroup the permutation group S_A , which permutes the spatial coordinates of a system of A particles.

The $Sp(3, \mathbb{R})$ scheme utilizes an important group reduction to classify many-particle basis states $|\sigma n \rho \omega \kappa LM\rangle$ of a symplectic irrep,

$$\begin{array}{ccccccc} Sp(3, \mathbb{R}) & \supset & U(3) & \supset & SO(3) & \supset & SO(2) \\ \sigma & & n\rho & & \omega & \kappa & L & M \end{array} \quad , \quad (6)$$

where $\sigma \equiv N_\sigma (\lambda_\sigma \mu_\sigma)$ labels the $Sp(3, \mathbb{R})$ irrep, $n \equiv N_n (\lambda_n \mu_n)$, $\omega \equiv N (\lambda_\omega \mu_\omega)$, and $N = N_\sigma + N_n$ is the total number of HO quanta (ρ and κ are multiplicity labels) [5]. The relation of these symplectic basis states to M -scheme states of the NCSM is provided in Ref. [43]. Importantly, a single-particle $Sp(3, \mathbb{R})$ irrep spans *all* positive-parity (or negative-parity) states for a particle in a three-dimensional spherical or triaxial (deformed) harmonic oscillator.

The translationally invariant (intrinsic) symplectic $Sp(3, \mathbb{R})$ generators can be written as $SU(3)$ tensor operators in terms of the harmonic oscillator raising, $b_{i\alpha}^{\dagger(10)} = \frac{1}{\sqrt{2}}(r_{i\alpha} - ip_{i\alpha})$, and lowering $b^{(01)}$ dimensionless operators (with \mathbf{r} and \mathbf{p} the laboratory-frame position and momentum coordinates and $\alpha = 1, 2, 3$ for the three spatial directions),

$$A_{\mathcal{LM}}^{(20)} = \frac{1}{\sqrt{2}} \sum_{i=1}^A \{b_i^\dagger \times b_i\}_{\mathcal{LM}}^{(20)} - \frac{1}{\sqrt{2}A} \sum_{s,t=1}^A \{b_s^\dagger \times b_t\}_{\mathcal{LM}}^{(20)} \quad (7)$$

$$C_{\mathcal{LM}}^{(11)} = \sqrt{2} \sum_{i=1}^A \{b_i^\dagger \times b_i\}_{\mathcal{LM}}^{(11)} - \frac{\sqrt{2}}{A} \sum_{s,t=1}^A \{b_s^\dagger \times b_t\}_{\mathcal{LM}}^{(11)},$$

$$H_{00}^{(00)} = \sqrt{3} \sum_i \{b_i^\dagger \times b_i\}_{00}^{(00)} - \frac{\sqrt{3}}{A} \sum_{s,t} \{b_s^\dagger \times b_t\}_{00}^{(00)} + \frac{3}{2}(A-1), \quad (8)$$

together with $B_{\mathcal{LM}}^{(02)} = (-)^{\mathcal{L}-M} (A_{\mathcal{L}-M}^{(20)})^\dagger$ ($\mathcal{L} = 0, 2$), where the sums run over all A particles of the system. Equivalently, the symplectic generators, being one-body-plus-two-body operators can be expressed in terms of the fermion creation operator $a_{(\eta 0)}^\dagger$ and its $SU(3)$ -conjugate annihilation operator, $\tilde{a}_{(0 \eta)}$. This is achieved by using the known matrix elements of the position and momentum operators in a HO basis, and hence, e.g., the first sum of $A_{\mathcal{LM}}^{(20)}$ in Eq. (7) becomes, $\sum_\eta \sqrt{\frac{(\eta+1)(\eta+2)(\eta+3)(\eta+4)}{12}} \left\{ a_{(\eta+2 0)}^\dagger \times \tilde{a}_{(0 \eta)} \right\}_{\mathcal{LM}}^{(20)}$ [44]. Note that this operator describes excitations of a nucleon from the η shell to the $\eta + 2$ shell, which corresponds to creating two single-particle HO excitation quanta, as manifested in the first term of Eq. (7). The eight $0\hbar\Omega$ operators $C_{\mathcal{L},M}^{(11)}$ ($\mathcal{L} = 1, 2$) generate the $SU(3)$ subgroup of $Sp(3, \mathbb{R})$. They realize the angular momentum operator (dimensionless), $L_{1M} = C_{1M}^{(11)}$, and the Elliott “algebraic” quadrupole moment tensor $Q_{2M}^a = \sqrt{3} C_{2M}^{(11)}$.

The many-body basis states of an $Sp(3, \mathbb{R})$ irrep are built over a bandhead $|\sigma\rangle$ (defined by the usual requirement that the symplectic lowering operators $B_{\mathcal{LM}}^{(02)}$ annihilate it) by $2\hbar\Omega$ 1p-1h monopole or quadrupole excitations, realized by the first term in $A_{\mathcal{LM}}^{(20)}$ of Eq. (7), together

193 with a smaller $2\hbar\Omega$ 2p-2h correction for eliminating the spurious center-of-mass (CM) motion,
 194 realized by the second term in $A_{\mathcal{L}M}^{(20)}$:

$$|\sigma n \rho \omega \kappa (LS_\sigma) JM\rangle = \sum_{M_L M_S} \langle LM_L; S_\sigma M_S | JM \rangle \{ \{ A^{(20)} \times A^{(20)} \dots \times A^{(20)} \}^n \times |\sigma; S_\sigma M_S\rangle \}_{\kappa LM_L}^{\rho \omega}. \quad (9)$$

195 States within a symplectic irrep have the same spin value, which are given by the spin S_σ
 196 of the bandhead $|\sigma; S_\sigma\rangle$. Symplectic basis states span the entire shell-mode space. A com-
 197 plete set of labels includes additional quantum numbers $|\{\alpha\}\sigma\rangle$ that distinguish different
 198 bandheads with the same N_σ ($\lambda_\sigma \mu_\sigma$). Remarkably, these $\text{Sp}(3, \mathbb{R})$ basis states are in one-
 199 to-one correspondence with a coupled product of the states of the Bohr vibrational model
 200 (realized in terms of giant monopole-quadrupole resonance states with irrotational flows),
 201 $\{ \{ A^{(20)} \times A^{(20)} \dots \times A^{(20)} \}^n \times |N_\sigma(00)\rangle \}^{(\lambda_n \mu_n)}$, and $(\lambda_\sigma \mu_\sigma)$ deformed states of an $\text{SU}(3)$
 202 model [42].

203 2.3 *Ab initio* symmetry-adapted no-core shell model

204 Not surprisingly, the symplectic $\text{Sp}(3, \mathbb{R})$ symmetry, the underlying symmetry of the symplectic
 205 rotor model [3, 5], has been found to play a key role across the nuclear chart – from the lightest
 206 systems [45, 46], through intermediate-mass nuclei [4, 47, 8], up to strongly deformed nuclei
 207 of the rare-earth and actinide regions [5, 48, 49, 19]. The results agree with experimental
 208 evidence that supports formation of enhanced deformation and clusters in nuclei, as well as
 209 vibrational and rotational patterns, as suggested by energy spectra, electric monopole and
 quadrupole transitions, radii and quadrupole moments [11, 29, 50].

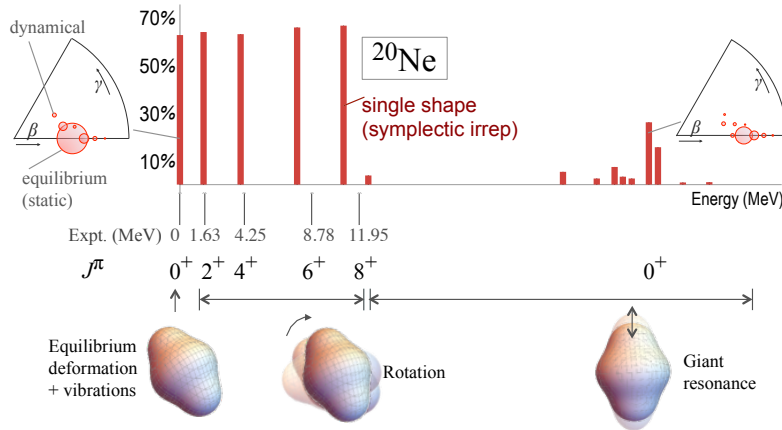


Figure 1: Emergence of almost perfect symplectic $\text{Sp}(3, \mathbb{R})$ symmetry in nuclei from first principles, enabling *ab initio* descriptions of collectivity and clustering. *Source:* Figure from [2] @ APS; reproduced with permission.

210 The symmetry-adapted no-core shell model [20, 8, 2] capitalizes on these findings and
 211 presents solutions in terms of a physically relevant basis of nuclear shapes. It exploits both
 212 the $\text{SU}(3)$ and $\text{Sp}(3, \mathbb{R})$ schemes. Indeed, since the symplectic symmetry does not mix nuclear
 213 shapes, the SA-NCSM provides important insight from first principles into the physics of nuclei
 214 and their low-lying excitations as dominated by only a few (typically one or two) collective
 215 shapes – equilibrium shapes with their vibrations – that rotate (Fig. 1).
 216

217 By exploiting this almost perfect symmetry, the SA framework resolves the scale explo-
 218 sion problem in nuclear structure calculations, *i.e.*, the explosive growth in computational
 219 resource demands with increasing number of particles and model spaces size. We note that

the SA-NCSM uses the complete model space (that is, all possible shapes) as usually done in conventional shell models, but expands, in a prescribed way, only for those deformed configurations with vibrations that lie outside of the complete model space. This is critical for enhanced prolate deformation, since spherical and less deformed or oblate shapes easily develop in comparatively small model-space sizes.

The SA-NCSM, when combined with a high-precision realistic inter-nucleon interaction, provides *ab initio* predictions of nuclear observables. We often adopt the NNLO_{opt} chiral potential [51] that is used without 3N forces, which have been shown to contribute minimally to the 3- and 4-nucleon binding energy [51]. Chiral potentials are typically parameterized by two-nucleon (and three-nucleon) data, whereas the parameters, called the low-energy constants (LECs), remain unchanged and are not adjusted from one many-body system to another. This ensures a predictive power. At the next-to-next-to-leading order (NNLO), there are 14 LECs that enter into the chiral nucleon-nucleon (NN) potential. Our recent findings reveal the remarkable result that the chiral potential parameterizations have no significant effect on the dominant nuclear features, such as nuclear shape and the associated Sp(3, \mathbb{R}) symmetry, along with cluster formation (Fig. 2), but only slightly vary details in the nuclear wave functions, such as the contributions of the equilibrium deformation and its vibrations within the predominant nuclear shape (Fig. 2, left, inset) [52].

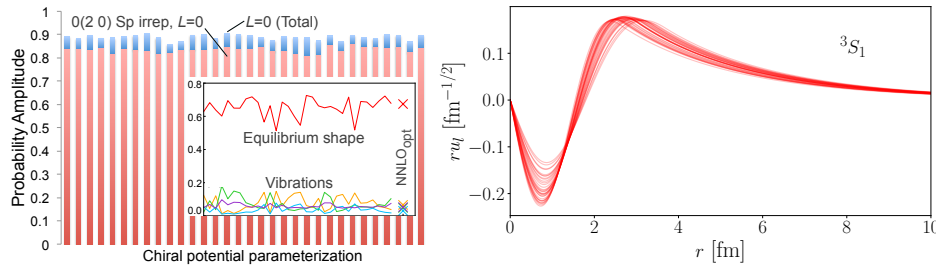


Figure 2: Chiral parameterization independence for nuclear shapes and cluster formation: (Left) Probability amplitude of the predominant Sp(3, \mathbb{R}) irrep $N_\sigma(\lambda_\sigma \mu_\sigma) = 0(20)$ ($L = 0$) in the ${}^6\text{Li } 1^+$ ground state. Inset: Contributions from the equilibrium shape (symplectic bandhead) and its vibrations (the case for the NNLO_{opt} is also shown). (Right) $\alpha + d$ 3S_1 -wave vs. the relative distance r . Calculated from the ${}^6\text{Li } 1^+$ ground state, computed with the SA-NCSM in the Sp(3, \mathbb{R}) scheme with NNLO chiral potential for 10 HO shells and $\hbar\Omega=15$ MeV. The $\pm 10\%$ variation in the LECs of the chiral potential is shown (left) on the horizontal axis and (right) by the spread of the curve. *Source:* Figures adapted/reused from [52] @ Frontiers; reproduced under the terms of its CC BY license.

3 Critical Role of Symmetries for Studies and Predictions of Nuclear Properties

3.1 Machine learning pattern recognition with the SA-NCSM

Machine learning approaches are ideal for pattern recognition, thereby providing a suitable framework to detect and utilize the highly organized patterns in atomic nuclei governed by the symplectic Sp(3, \mathbb{R}) symmetry.

Specifically, Ref. [32] introduces a novel machine learning approach to provide further

insight into atomic nuclei and to detect orderly patterns amidst a vast data of large-scale calculations. The method utilizes a physics-informed neural network that is trained on *ab initio* results from the SA-NCSM for light nuclei. Indeed, the SA-NCSM, which expands *ab initio* applications up to medium-mass nuclei, can reach even heavier nuclei when coupled with the machine learning approach. In particular, we find that a neural network trained on probability amplitudes for *s*- and *p*-shell nuclear wave functions not only predicts dominant configurations for heavier nuclei but in addition, when tested for the ^{20}Ne ground state, it accurately reproduces the probability distribution (Fig. 3).

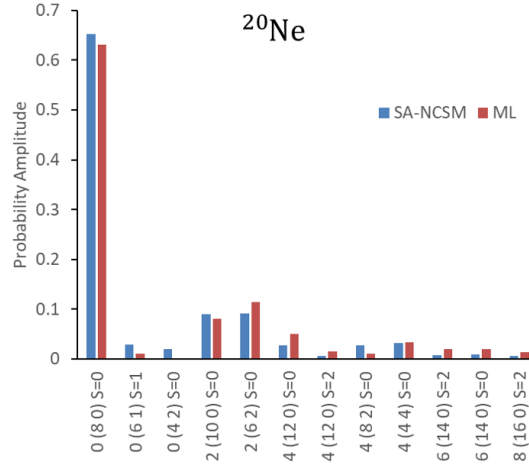


Figure 3: A novel machine learning approach coupled with the *ab initio* SA-NCSM is capable to detect orderly patterns amidst a vast data of large-scale calculations and to describe *sd*-shell nuclei, such as ^{20}Ne (shown), ^{24}Si , ^{40}Mg , and even the extremely heavy nuclei such as $^{166,168}\text{Er}$ and ^{236}U , by training only on nuclei up to ^{16}O . *Source:* Figure from [32] @ APS; reproduced with permission.

The nonnegligible configurations predicted by the network provide an important input to the SA-NCSM for reducing ultra-large model spaces to manageable sizes that can be, in turn, utilized in SA-NCSM calculations to obtain accurate observables. The neural network is capable of describing nuclear deformation and is used to track the shape evolution along the $^{20-42}\text{Mg}$ isotopic chain, suggesting a shape-coexistence that is more pronounced toward the very neutron-rich isotopes [32]. Furthermore, the neural network provides first descriptions of the structure and deformation of ^{24}Si and ^{40}Mg of interest to x-ray burst nucleosynthesis, and even of the extremely heavy nuclei such as $^{166,168}\text{Er}$ and ^{236}U , that build upon first principles considerations [32].

3.2 Probing clustering and physics beyond the standard model

The left-handed vector minus axial-vector (*V*–*A*) structure of the weak interaction was postulated in late 1950's and early 1960's guided in large part by a series of beta-decay experiments, and later was incorporated in the Standard Model of particle physics. However, in its most general form, the weak interaction can also have scalar, tensor, and pseudoscalar terms as well as right-handed currents. The β decay of ^8Li to ^8Be , which subsequently breaks up into two α particles, has long been recognized as an excellent testing ground to search for new physics (e.g. see [53]) due to the high decay energy and the ease of detecting the β and two α particles. These experiments have achieved remarkable precision (e.g., see [54,55]) that now

271 requires confronting the systematic uncertainties that stem from the higher-order corrections
in nuclear beta decay that are difficult to measure experimentally.

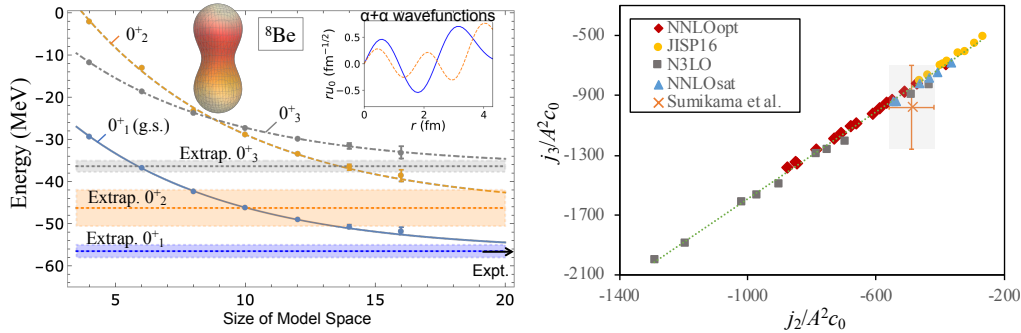


Figure 4: The *ab initio* SA-NCSM places unprecedented constraints on higher-(recoil-) order corrections (j_2/A^2c_0 and j_3/A^2c_0) in the β decay of ${}^8\text{Li} \rightarrow {}^8\text{Be}$ by addressing the challenging $\alpha + \alpha$ structure of ${}^8\text{Be}$. The results are essential for largely improving the sensitivity of high-precision experiments that probe the weak interaction theory and test physics beyond the Standard Model [55, 33]. Calculations performed on the NERSC and Frontera HPC systems. *Source:* Figures from [33] @ APS; reproduced with permission.

272

273

274 As a remarkable result, the *ab initio* SA-NCSM has recently determined the size of the
275 recoil-order form factors in the β decay of ${}^8\text{Li}$ (Fig. 4). It has shown that states of the $\alpha + \alpha$
276 system not included in the evaluated ${}^8\text{Be}$ energy spectrum have an important effect on all
277 $j_{2,3}/A^2c_0$, b/Ac_0 and d/Ac_0 recoil-order terms, and can explain the elusive M_{GT} discrepancy in
the $A = 8$ systems common to all other *ab initio* approaches.

278

279 The SA-NCSM outcomes of Ref. [33] reduce – by over 50% – the uncertainty on these
280 recoil-order corrections. These results help improve the sensitivity of high-precision β -decay
281 experiments that probe the V–A structure of the weak interaction in the most stringent limit
282 on tensor current contribution to the weak interaction theory to date, established in Ref. [55].
283 Furthermore, the SA-NCSM predicted b/Ac_0 and d/Ac_0 values are important for other inves-
284 tigations of the Standard Model symmetries, such as the conserved vector current hypothesis
and the existence of second-class currents in the weak interaction.

285 3.3 Optical potential in the symmetry-adapted framework for nuclear reactions

286 In recent years there has been a significant interest in describing nuclear reactions from *ab*
287 *initio* approaches, and especially in constructing from first principles effective inter-cluster
288 interactions, often referred to as optical potentials. *Ab initio* optical potentials for elastic
289 scattering at low energy are of particular interest for experiments at rare isotope beams. To
290 utilize the efficacy of the symmetry-adapted basis, we combine the *ab initio* symmetry-adapted
291 no-core shell model with the Green’s function technique (SANCSM/GF) and construct non-
292 local optical potentials rooted in first principles [56, 57]. Using the Green’s function technique
293 ensures that all relevant cluster partitionings are included in the effective potential between
294 the two reaction fragments (clusters) that are typically in their ground state in the entrance
295 channel. With the view toward studying neutron and proton elastic scattering from deformed
296 and heavy targets, we first examine a target of ${}^4\text{He}$ (Fig. 5a), where the effect of the spurious
297 center-of-mass motion is most evident.

298 In a complementary symmetry-adapted resonating group method (SA-RGM) framework
299 [58], one starts from an *ab initio* description of all particles involved and derives the effec-
300 tive potential for localized clusters, which are properly normalized and orthogonalized in the

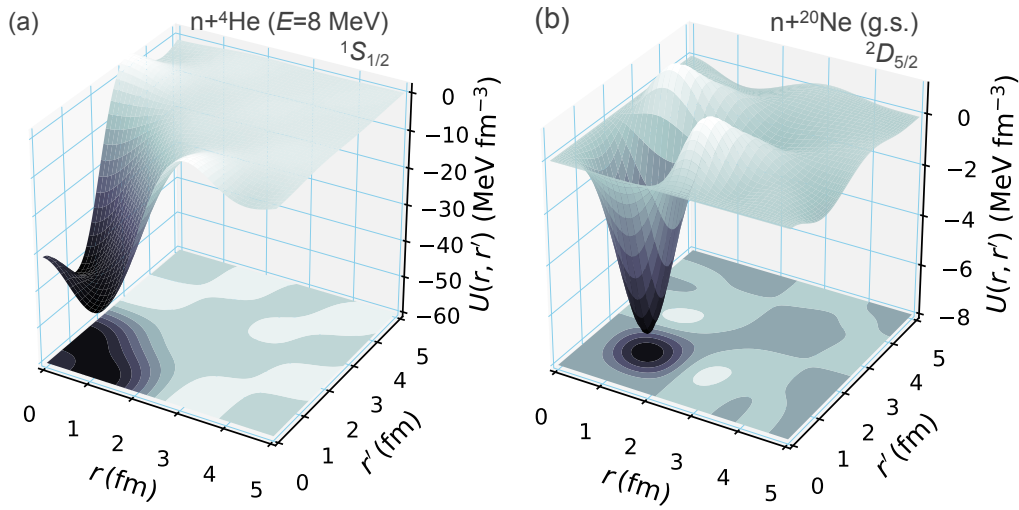


Figure 5: (a) Translationally invariant non-local optical potential for elastic neutron scattering for a ${}^4\text{He}$ target at $E = 8$ MeV center-of-mass energy, calculated in the SA-NCSM with the Green's function technique (10 shells, $\hbar\Omega=17\text{MeV}$). Figure from [56]. (b) Effective neutron-nucleus non-local potential (translationally invariant) for the ${}^{20}\text{Ne}$ ground state, where effects of the target excitations and antisymmetrization involving three nucleons are neglected (based on *ab initio* SA-NCSM calculations of ${}^{20}\text{Ne}$ with NNLO_{opt} in a model space of 11 shells and $\hbar\Omega=15$ MeV inter-shell distance). Source: Figure from [1] @ Annual Reviews; reproduced under the terms of its CC BY license.

particle sector, which yields non-local effective nucleon-nucleus interactions for the cluster partitioning or channel under consideration. For a single channel, if the effects of the target excitations are neglected, the non-local effective nucleon-nucleus interaction can be calculated for each partial wave, as illustrated for $n+{}^{20}\text{Ne}(0_{\text{g.s.}}^+)$ with NNLO_{opt} in 11 shells (Fig. 5b). While these calculations limit the antisymmetrization to two nucleons only, this is a first step toward constructing effective nucleon-nucleus potentials for light and medium-mass nuclei for the astrophysically relevant energies [59, 60].

4 Conclusion

We have discussed the critical role of the emergent $\text{Sp}(3, \mathbb{R})$ symmetry in atomic nuclei and the associated subgroup $\text{SU}(3)$, which in turn underpin the $\text{Sp}(3, \mathbb{R})$ and $\text{SU}(3)$ schemes. By exploiting these schemes, the *ab initio* SA-NCSM has enabled machine-learning pattern recognition and descriptions of heavy nuclei, *ab initio* modeling of α clustering and collectivity, along with tests of beyond-the-standard-model physics. In addition, we show that with the help of the SA-NCSM, which expands *ab initio* applications up to medium-mass nuclei by using the dominant symmetry of nuclear dynamics, one can provide solutions to reaction processes in this region, with a focus on elastic neutron scattering.

Acknowledgements

We are grateful to J. E. Escher, A. Ekström, D. Rowe, G. Rosensteel, and J. Wood for useful discussions, as well as to N.D. Scielzo, M.T. Burkey, A.T. Gallant, G. Savard, and collaborators for motivating and providing important insights on the ^8Li decay study.

Funding information This work was supported in part by the U.S. National Science Foundation (PHY-1913728, PHY-2209060), the U.S. Department of Energy (DE-SC0019521, DE-SC0023532) and the Czech Science Foundation (22-14497S). This work was performed under the auspices of the U.S. Department of Energy by Lawrence Livermore National Laboratory under Contract DE-AC52-07NA27344 and the National Nuclear Security Administration through the Center for Excellence in Nuclear Training and University Based Research (CENTAUR) under Grant No. DE-NA0003841. This work benefited from high performance computational resources provided by LSU (www.hpc.lsu.edu), the National Energy Research Scientific Computing Center (NERSC), a U.S. Department of Energy Office of Science User Facility operated under Contract No. DE-AC02-05CH11231, as well as the Frontera computing project at the Texas Advanced Computing Center, made possible by National Science Foundation award OAC-1818253.

References

- [1] K. D. Launey, A. Mercenne and T. Dytrych, *Nuclear dynamics and reactions in the ab initio symmetry-adapted framework*, Annu. Rev. Nucl. Part. Sci. **71**, 253 (2021), doi:[10.1146/annurev-nucl-102419-033316](https://doi.org/10.1146/annurev-nucl-102419-033316).
- [2] T. Dytrych, K. D. Launey, J. P. Draayer, D. J. Rowe, J. L. Wood, G. Rosensteel, C. Bahri, D. Langr and R. B. Baker, *Physics of nuclei: Key role of an emergent symmetry*, Phys. Rev. Lett. **124**, 042501 (2020), doi:[10.1103/PhysRevLett.124.042501](https://doi.org/10.1103/PhysRevLett.124.042501).
- [3] G. Rosensteel and D. J. Rowe, *Nuclear Sp(3,R) Model*, Phys. Rev. Lett. **38**, 10 (1977).
- [4] J. Draayer, K. Weeks and G. Rosensteel, *Symplectic Shell-model Calculations for ^{20}Ne with Horizontal Configuration Mixing*, Nucl. Phys. **A413**, 215 (1984).
- [5] D. J. Rowe, *Microscopic theory of the nuclear collective model*, Reports on Progr. in Phys. **48**, 1419 (1985).
- [6] J. P. Draayer and Y. Akiyama, *Wigner and Racah Coefficients for SU(3)*, J. Math. Phys. **14**, 1904 (1973).
- [7] A. Blokhin, C. Bahri and J. Draayer, *Origin of pseudospin symmetry*, Phys. Rev. Lett. **74**, 4149 (1995).
- [8] K. D. Launey, T. Dytrych and J. P. Draayer, *Symmetry-guided large-scale shell-model theory*, Prog. Part. Nucl. Phys. **89**, 101 (review) (2016), doi:[10.1016/j.ppnp.2016.02.001](https://doi.org/10.1016/j.ppnp.2016.02.001).
- [9] G. Rosensteel and D. J. Rowe, *On the algebraic formulation of collective models iii. the symplectic shell model of collective motion*, Ann. Phys. N.Y. **126**, 343 (1980).
- [10] D. J. Rowe, *Dynamical symmetries of nuclear collective models*, Prog. Part. Nucl. Phys. **37**, 265 (1996).

- [11] K. Heyde and J. L. Wood, *Shape coexistence in atomic nuclei*, Rev. Mod. Phys. **83**, 1467 (2011).
- [12] J. L. Wood, *Nuclear Collectivity – its emergent nature viewed from phenomenology and spectroscopy*, In *Emergent phenomena in atomic nuclei from large-scale modeling: a symmetry-guided perspective*, p. 3. World Scientific Publishing Co., ISBN 978-981-3146-04-4, 978-981-3146-06-8, doi:[10.1142/9789813146051_0001](https://doi.org/10.1142/9789813146051_0001) (2017).
- [13] D. J. Rowe and J. L. Wood, *A relationship between isobaric analog states and shape coexistence in nuclei*, J. Phys. G: Nucl. Part. Phys. **45**(6), 06LT01 (2018).
- [14] J. P. Elliott, *Collective Motion in the Nuclear Shell Model. I. Classification Schemes for States of Mixed Configurations*, Proc. Roy. Soc. A **245**, 128 (1958).
- [15] J. P. Elliott, *Collective Motion in the Nuclear Shell Model. II. The Introduction of Intrinsic Wave-Functions*, Proc. Roy. Soc. A **245**, 562 (1958).
- [16] J. P. Elliott and M. Harvey, *Collective Motion in the Nuclear Shell Model. III. The Calculation of Spectra*, Proc. Roy. Soc. A **272**, 557 (1963).
- [17] K. T. Hecht and A. Adler, *Generalized seniority for favored $J \neq 0$ pairs in mixed configurations*, Nucl. Phys. A **A137**, 129 (1969).
- [18] K. T. Hecht and W. Zahn, *An $SU(3)$ approach to nuclear multi-cluster problems*, Nucl. Phys. A **318**, 1 (1979).
- [19] C. Bahri and D. J. Rowe, *$Su(3)$ quasi-dynamical symmetry as an organizational mechanism for generating nuclear rotational motions*, Nucl. Phys. A **662**, 125 (2000).
- [20] T. Dytrych, K. D. Sviratcheva, C. Bahri, J. P. Draayer and J. P. Vary, *Evidence for Symplectic Symmetry in ab initio No-core-shell-model Results for Light Nuclei*, Phys. Rev. Lett. **98**, 162503 (2007).
- [21] T. Dytrych, K. D. Launey, J. P. Draayer, P. Maris, J. P. Vary, E. Saule, U. Catalyurek, M. Sosonkina, D. Langr and M. A. Caprio, *Collective Modes in Light Nuclei from First Principles*, Phys. Rev. Lett. **111**, 252501 (2013), doi:[10.1103/PhysRevLett.111.252501](https://doi.org/10.1103/PhysRevLett.111.252501).
- [22] P. F. Bedaque and U. van Kolck, *Effective field theory for few-nucleon systems*, Annu. Rev. Nucl. Part. Sci. **52**(1), 339 (2002), doi:[10.1146/annurev.nucl.52.050102.090637](https://doi.org/10.1146/annurev.nucl.52.050102.090637).
- [23] E. Epelbaum, A. Nogga, W. Glöckle, H. Kamada, U.-G. Meißner and H. Witala, *Three-nucleon forces from chiral effective field theory*, Phys. Rev. C **66**, 064001 (2002).
- [24] D. R. Entem and R. Machleidt, *Accurate charge-dependent nucleon-nucleon potential at fourth order of chiral perturbation theory*, Phys. Rev. C **68**, 041001(R) (2003).
- [25] T. Dytrych, P. Maris, K. D. Launey, J. P. Draayer, J. P. Vary, M. Caprio, D. Langr, U. Catalyurek and M. Sosonkina, *Efficacy of the $SU(3)$ scheme for ab initio large-scale calculations beyond the lightest nuclei*, Comput. Phys. Commun. **207**, 202 (2016), doi:[10.1016/j.cpc.2016.06.006](https://doi.org/10.1016/j.cpc.2016.06.006).
- [26] T. Dytrych, A. C. Hayes, K. D. Launey, J. P. Draayer, P. Maris, J. P. Vary, D. Langr and T. Oberhuber, *Electron-scattering form factors for ${}^6\text{Li}$ in the ab initio symmetry-guided framework*, Phys. Rev. C **91**, 024326 (2015), doi:[10.1103/PhysRevC.91.024326](https://doi.org/10.1103/PhysRevC.91.024326).

- [27] R. B. Baker, K. D. Launey, S. Bacca, N. N. Dinur and T. Dytrych, *Benchmark calculations of electromagnetic sum rules with a symmetry-adapted basis and hyperspherical harmonics*, Phys. Rev. C **102**, 014320 (2020), doi:[10.1103/PhysRevC.102.014320](https://doi.org/10.1103/PhysRevC.102.014320).
- [28] P. Ruotsalainen, J. Henderson, G. Hackman, G. H. Sargsyan, K. D. Launey, A. Saxena, P. C. Srivastava, S. R. Stroberg, T. Grahm, J. Pakarinen, G. C. Ball, R. Julin *et al.*, *Isospin symmetry in $b(e2)$ values: Coulomb excitation study of ^{21}Mg* , Phys. Rev. C **99**, 051301 (2019), doi:[10.1103/PhysRevC.99.051301](https://doi.org/10.1103/PhysRevC.99.051301).
- [29] J. Henderson *et al.*, *Testing microscopically derived descriptions of nuclear collectivity: Coulomb excitation of ^{22}Mg* , Phys. Lett. **B782**, 468 (2018), doi:[10.1016/j.physletb.2018.05.064](https://doi.org/10.1016/j.physletb.2018.05.064), [1709.03948](https://arxiv.org/abs/1709.03948).
- [30] J. Williams, G. C. Ball, A. Chester, T. Domingo, A. B. Garnsworthy, G. Hackman, J. Henderson, R. Henderson, R. Krücken, A. Kumar, K. D. Launey, J. Measures *et al.*, *Structure of ^{28}Mg and influence of the neutron pf shell*, Phys. Rev. C **100**, 014322 (2019), doi:[10.1103/PhysRevC.100.014322](https://doi.org/10.1103/PhysRevC.100.014322).
- [31] K. D. Launey, A. Mercenne, G. H. Sargsyan, H. Shows, R. B. Baker, M. E. Miora, T. Dytrych and J. P. Draayer, *Emergent clustering phenomena in the framework of the *ab initio* symmetry-adapted no-core shell model*, In *Proceedings of the 4th International Workshop on 'State of the Art in Nuclear Cluster Physics' (SOTANCP4), May 2018, Galveston, Texas*, vol. 2038. AIP Conference Proceedings (2018).
- [32] O. M. Molchanov, K. D. Launey, A. Mercenne, G. H. Sargsyan, T. Dytrych and J. P. Draayer, *Machine learning approach to pattern recognition in nuclear dynamics from the *ab initio* symmetry-adapted no-core shell model*, Phys. Rev. C **105**, 034306 (2022), doi:[10.1103/PhysRevC.105.034306](https://doi.org/10.1103/PhysRevC.105.034306).
- [33] G. H. Sargsyan, K. D. Launey, M. T. Burkey, A. T. Gallant, N. D. Scielzo, G. Savard, A. Mercenne, T. Dytrych, D. Langr, L. Varriano, B. Longfellow, T. Y. Hirsh *et al.*, *Impact of clustering on the ^8Li β decay and recoil form factors*, Phys. Rev. Lett. **128**, 202503 (2022), doi:[10.1103/PhysRevLett.128.202503](https://doi.org/10.1103/PhysRevLett.128.202503).
- [34] M. Moshinsky, *Wigner Coefficients for the SU_3 Group and Some Applications*, Rev. Mod. Phys. **34**, 813 (1962).
- [35] M. Moshinsky, J. Patera, R. T. Sharp and P. Winternitz, *Everything you always wanted to know about $SU(3) \supset O(3)$* , Ann. Phys. (N.Y.) **95**, 139 (1975).
- [36] V. K. B. Kota, *$SU(3)$ Symmetry in Atomic Nuclei*, Springer Singapore, ISBN 978-981-15-3602-1, doi:[10.1007/978-981-15-3603-8](https://doi.org/10.1007/978-981-15-3603-8) (2020).
- [37] G. Rosensteel and D. J. Rowe, *On the shape of deformed nuclei*, Ann. Phys. N.Y. **104**, 134 (1977).
- [38] Y. Leschber and J. P. Draayer, *Algebraic realization of rotational dynamics*, Phys. Letts. B **190**, 1 (1987).
- [39] O. Castaños, J. P. Draayer and Y. Leschber, *Shape variables and the shell model*, Z. Phys. A **329**, 33 (1988).
- [40] D. J. Rowe and J. L. Wood, *Fundamentals of nuclear models: foundational models*, World Scientific, Singapore (2010).

- [41] J. P. Draayer, Y. Leschber, S. C. Park and R. Lopez, *Representations of $U(3)$ in $U(N)$* , Comput. Phys. Commun. **56**, 279 (1989).
- [42] D. Rowe, *The fundamental role of symmetry in nuclear models*, AIP Conf. Proc. **1541**, 104 (2013).
- [43] T. Dytrych, K. D. Sviratcheva, J. P. Draayer, C. Bahri and J. P. Vary, *Ab initio symplectic no-core shell model*, J. Phys. G: Nucl. Part. Phys. **35**, 123101 (2008).
- [44] J. Escher and J. P. Draayer, *Fermion realization of the nuclear $sp(6,r)$ model*, J. Math. Phys. **39**, 5123 (1998).
- [45] D. J. Rowe, G. Thiamova and J. L. Wood, *Implications of Deformation and Shape Coexistence for the Nuclear Shell Model*, Phys. Rev. Lett. **97**, 202501 (2006).
- [46] A. C. Dreyfuss, K. D. Launey, T. Dytrych, J. P. Draayer and C. Bahri, *Hoyle state and rotational features in Carbon-12 within a no-core shell model framework*, Phys. Lett. B **727**, 511 (2013).
- [47] G. K. Tobin, M. C. Ferriss, K. D. Launey, T. Dytrych, J. P. Draayer and C. Bahri, *Symplectic No-core Shell-model Approach to Intermediate-mass Nuclei*, Phys. Rev. C **89**, 034312 (2014).
- [48] O. Castaños, P. Hess, J. Draayer and P. Rochford, *Pseudo-symplectic model for strongly deformed heavy nuclei*, Nucl. Phys. A **524**, 469 (1991).
- [49] M. Jarrío, J. L. Wood and D. J. Rowe, *The $SU(3)$ structure of rotational states in heavy deformed nuclei*, Nucl. Phys. A **528**, 409 (1991).
- [50] M. Freer, H. Horiuchi, Y. Kanada-En'yo, D. Lee and U.-G. Meißner, *Microscopic clustering in light nuclei*, Rev. Mod. Phys. **90**, 035004 (2018), doi:[10.1103/RevModPhys.90.035004](https://doi.org/10.1103/RevModPhys.90.035004).
- [51] A. Ekström, G. Baardsen, C. Forssén, G. Hagen, M. Hjorth-Jensen, G. R. Jansen, R. Machleidt, W. Nazarewicz *et al.*, *An optimized chiral nucleon-nucleon interaction at next-to-next-to-leading order*, Phys. Rev. Lett. **110**, 192502 (2013).
- [52] K. S. Becker, K. D. Launey, A. Ekstrom and T. Dytrych, *Ab initio symmetry-adapted emulator for studying emergent collectivity and clustering in nuclei*, Front. Phys. **11**, 1064601 (2023), doi:[10.3389/fphy.2023.1064601](https://doi.org/10.3389/fphy.2023.1064601).
- [53] B. R. Holstein, *Recoil effects in allowed beta decay: The elementary particle approach*, Rev. Mod. Phys. **46**, 789 (1974), doi:[10.1103/RevModPhys.46.789](https://doi.org/10.1103/RevModPhys.46.789).
- [54] M. Sternberg, R. Segel, N. Scielzo, G. Savard, J. Clark, P. Bertone, F. Buchinger, M. Burkey, S. Caldwell, A. Chaudhuri *et al.*, *Limit on tensor currents from ^8Li β decay*, Phys. Rev. Lett. **115**(18), 182501 (2015).
- [55] M. T. Burkey, G. Savard, A. T. Gallant, N. D. Scielzo, J. A. Clark, T. Y. Hirsh, L. Varriano, G. H. Sargsyan, K. D. Launey, M. Brodeur, D. P. Burdette, E. Heckmaier *et al.*, *Improved limit on tensor currents in the weak interaction from ^8Li β decay*, Phys. Rev. Lett. **128**, 202502 (2022), doi:[10.1103/PhysRevLett.128.202502](https://doi.org/10.1103/PhysRevLett.128.202502).
- [56] M. B. Burrows, K. D. Launey *et al.*, *Ab initio low-energy optical potentials from the symmetry-adapted no-core shell model*, (in preparation) (2022).

- 475 [57] M. B. Burrows, K. D. Launey *et al.*, *Ab initio optical potentials for elastic scattering at low*
476 *energies using the symmetry-adapted no-core shell model*, 2021 Fall Meeting of the Divi-
477 sion of Nuclear Physics, APS (meetings.aps.org/Meeting/DNP21/Session/KM.3)
478 (2021).
- 479 [58] A. Mercenne, K. Launey, T. Dytrych, J. Escher, S. Quaglioni, G. Sargsyan, D. Langr and
480 J. Draayer, *Efficacy of the symmetry-adapted basis for ab initio nucleon-nucleus interactions*
481 *for light- and intermediate-mass nuclei*, Computer Physics Communications **280**, 108476
482 (2022), doi:<https://doi.org/10.1016/j.cpc.2022.108476>.
- 483 [59] A. Mercenne, K. D. Launey, J. E. Escher, T. Dytrych and J. P. Draayer, *New Ab Initio*
484 *Approach to Nuclear Reactions Based on the Symmetry-Adapted No-Core Shell Model*, In
485 N. Orr, M. Ploszajczak, F. Marques and J. Carbonell, eds., *Recent Progress in Few-Body*
486 *Physics*, vol. 238, p. 253. Springer Proc. Phys., doi:[https://doi.org/10.1007/978-3-030-](https://doi.org/10.1007/978-3-030-32357-8_44)
487 [32357-8_44](https://doi.org/10.1007/978-3-030-32357-8_44) (2020).
- 488 [60] A. Mercenne, K. D. Launey, J. E. Escher, T. Dytrych and J. P. Draayer, *New ab initio ap-*
489 *proach to nuclear reactions based on the symmetry-adapted no-core shell model*, In J. Es-
490 cher, ed., *Proceedings of the 6th International Workshop on Compound-Nuclear Reactions*
491 *and Related Topics (CNR*18)*, p. 73. Berlin: Springer (2021).